ACS OMEGA

http://pubs.acs.org/journal/acsodf

Article

Analysis of the Distribution and Influencing Factors of Diffusion Coefficient Model Parameters Based on Molecular Dynamics Simulations

Wenting Sun, Xia Chen, Lianying Wu,* Yangdong Hu, and Weitao Zhang

Cite This: *ACS Omega* 2023, 8, 22536−22544

Read Online

ACCESS | Metrics & More | Article Recommendations | Supporting Information

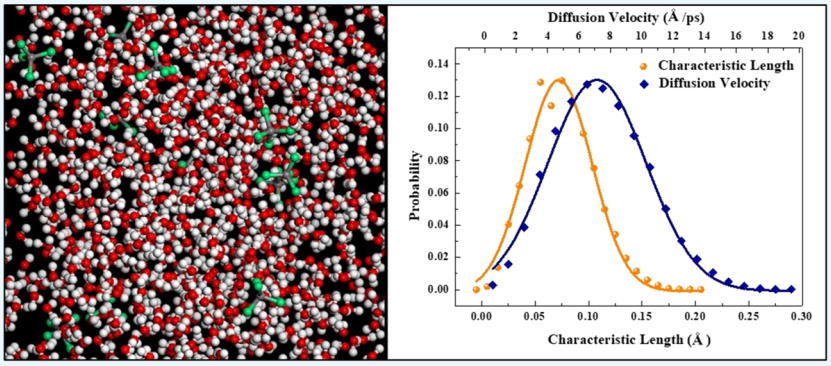

ABSTRACT: The establishment of mathematical models to predict the diffusion coefficients of gas and liquid systems have important theoretical significance and practical value. In this work, based on the previously proposed diffusion coefficient model D_{LV}, the distribution and influencing factors of the model parameters characteristic length (L) and diffusion velocity (V) were further investigated using molecular dynamics simulations. The statistical analysis of L and V for 10 gas systems and 10 liquid systems was presented in the paper. New distribution functions were established to describe the probability distributions of molecular motion L and V. The mean values of the correlation coefficients were 0.98 and 0.99, respectively. Meanwhile, the effects of molecular molar mass and system temperature on the molecular diffusion coefficients were discussed. The results show that the effect of molecular molar mass on the diffusion coefficient mainly affects the molecular motion L, and the effect of system temperature on the diffusion coefficient mainly affects V. For the gas system, the average relative deviation of D_{LV} and D_{MSD} is 10.73% and that of D_{LV} and experimental value is 12.63%; for the solution system, the average relative deviation of D_{LV} and D_{MSD} is 12.93% and that of D_{LV} and experimental value is 18.86%, which indicates the accuracy of the new model results. The new model reveals the potential mechanism of molecular motion and provides a theoretical basis for further study of the diffusion process.

1. INTRODUCTION

Diffusion is usually the rate-limiting step in chemical reactions and material separation, and the diffusion coefficient, as an important fundamental parameter reflecting the mass transfer capacity, is the key to the design and development of many processes.[1,2] The experimental determination and prediction of diffusion coefficients have important theoretical significance and practical value for revealing the mass transfer mechanism. For the measurement of the diffusion coefficient of gases, there are single-chamber methods and two-chamber methods.[3−5] For diffusion coefficients in mixed solution systems, the membrane cell method, Taylor dispersion method, optical interferometry, NMR method, etc., are usually used.[6−8] Although there have been more significant advances in experimental methods for measuring diffusion coefficients, the resolution of the experiments is usually low, preventing insight and access to more valid experimental data at the molecular level. After more than half a century of practice, molecular dynamics (MD) simulations have become a powerful tool for calculating diffusion coefficients, and since it describes real molecular motion, the role played by molecular parameters (e.g., molecular mass and intermolecular interactions) can be studied in detail.[9]

To obtain analytical results of molecular diffusion coefficients during the simulation, the researchers used various physical and mathematical models to predict the diffusion coefficients by optimizing the parameters.[10−14] In the previous work of our team, a new D_{LV} model was proposed to calculate the diffusion

Received: February 5, 2023
Accepted: April 18, 2023
Published: June 12, 2023

coefficient. We describe the diffusion coefficient as the product of the characteristic length L and the diffusion velocity V. The characteristic length (L) is defined as the average value of the diffusion distance, which is the distance that the moving molecule moves continuously without changing its direction. The diffusion velocity (V) is the average value of the molecular motion velocity. Through calculation and analysis, the prediction results of the new model were obtained in good agreement with the experimental results. And the results were obtained realistically and reliably when compared with the MSD model.[15,16] However, the statistical regularity of the model parameters and the mechanism of the effect of the nature of the diffusion system on the parameters and diffusion coefficients need to be further investigated. In the process of kinetic simulation calculations, many researchers have developed various open-source plug-ins to obtain accurate and effective results for properties such as diffusion coefficient and shear viscosity of pure fluids or mixtures.[17,18]

MD simulations have been widely used to study gas and liquid diffusion systems. Gas diffusion plays a key role in the study of gas absorption, transfer, etc. Economou, Panagiotopoulos, and their colleagues have made many contributions to molecular dynamics simulations. They calculated molecular diffusion in binary systems, including mixtures of carbon dioxide and water, carbon dioxide in various alkane systems such as hexane, various mixtures of alkanes and water, and aqueous salt mixtures, and obtained molecular transport properties at different temperature and pressure conditions.[19−23] Zhao et al. calculated the transfer and diffusion rates of CO_2 and CH_4 in coal seams by molecular simulation.[24] Rezlerovád et al. used molecular-level simulations to explore the adsorption, diffusion, and transport of methane, ethane, propane, and carbon dioxide at the temperature and pressure of typical shale reservoirs.[25] Higgoda et al. studied the self-diffusion coefficients of CH_4, CO_2, and C_3H_8 in superheated steam, gas, and supercritical states using the Einstein relation.[26,27] Classical MD methods were studied for binary aqueous systems. Klinov et al. calculated the diffusion coefficients in binary aqueous solutions of three alcohols.[28] Zhang et al. investigated the structural and diffusion properties of ethanol/water mixtures at 298.15 K and atmospheric pressure.[29] Moreover, the solution structures and diffusion coefficients of amino acids, vitamins, and other bioorganic substances in aqueous solutions have been systematically studied at different temperatures and concentrations.[30,31]

D_{LV} is a new model for calculating diffusion coefficients using molecular dynamics simulations. This model can obtain the diffusion coefficient by calculating the characteristic length (L) and diffusion velocity (V) of the molecules of the diffusion system. In this paper, we further investigate the statistical regularity of the model parameters L and V of the D_{LV} model of the diffusion coefficient and the mechanism by which the nature of the diffusion system affects the parameters and the diffusion coefficient and obtain the range of values of L and V and the value with the highest probability of occurrence through the probability distribution function. The microstructural properties of the fluid are obtained through this model simulation, and the nature of the diffusion phenomenon is revealed from the microscopic point of view, and the diffusion mechanism is obtained from the motion of the microscopic molecules at each step, providing a new perspective for the study of the diffusion coefficient.

2. MODELS AND SIMULATION TECHNIQUES

2.1. Model Description. In our previous work, a new diffusion coefficient model based on Fick's law was developed.[15] Fick's law mainly describes the relationship between the rate of molecular diffusion and the concentration gradient. The diffusion flux (j_A) can be expressed as

$$j_A = -D_{AB}\frac{d\rho_A}{d_y} \tag{1}$$

where $\frac{d\rho_A}{dy}$ is the mass concentration gradient and D_{AB} is the Fickian diffusion coefficient with the unit of $\frac{m^2}{s}$ (square meter per second).

According to the dimension analysis method

$$\frac{m^2}{s} = m \times \frac{m}{s} \tag{2}$$

Thus, the explicit physical meaning of Fick's law diffusion coefficient can be assumed to be the product of the characteristic length (L) and the diffusion velocity (V). As in eq 3

$$D_{LV} = L \times V \tag{3}$$

where D_{LV} denotes the diffusion coefficient, L denotes the characteristic length, and V denotes the diffusion velocity. Further, L is the statistical average of the molecular diffusion distance. V can be considered as the statistical average velocity of the molecular motion.

For comparison, we also used the mean square displacement (MSD) method to calculate the diffusion coefficient. The diffusion coefficient can be obtained according to the well-known Einstein equation (eq 4).[32,33]

$$D_{MSD} = \lim_{t\to\infty}\frac{1}{6Nt}\sum_{i}^{N}\langle |r_i(t) - r_i(t_0)|^2\rangle \tag{4}$$

where D_{MSD} denotes the diffusion coefficient, N is the number of penetrants, $r_i(t_0)$ and $r_i(t)$ are the initial and final positions of the center of mass of penetrant i over the time interval t, and $\langle |r_i(t) - r_i(t_0)|^2\rangle$ is the average mean square displacement. The diffusion coefficient was determined from the slope of MSD versus time data.

To avoid the effect of the finite size effect of the system on the simulation results, Yeh and Hummer estimated the specific hydrodynamic self-interaction caused by periodic boundary conditions from the difference of Oseen tensor in finite periodic and infinite nonperiodic systems, and in this paper, the Yeh−Hummer correction was used to correct the D_{LV} and D_{MSD} for the liquid system.[34−36] The gas system was chosen to simulate 1000 molecules to avoid errors caused by system size.[16]

$$D_{MSD-cd} = D_{MSD} + D_{YH} \tag{5}$$

$$D_{LV-cd} = D_{LV} + D_{YH} \tag{6}$$

$$D_{YH} = \frac{k_B T\xi}{6\pi\eta L_i} \tag{7}$$

where $D_{MSD\text{-}cd}$ is the corrected D_{MSD}, D_{YH} is the Yeh−Hummer correction diffusivity, and $D_{LV\text{-}cd}$ is the corrected D_{LV}. k^B is the Boltzmann constant, T is the temperature, η is the shear viscosity, L_i is the length of the cubic simulation box, and ξ is a constant that depends on the shape of the simulation box (for a cubic simulation box, $\xi = 2.837297$).

https://doi.org/10.1021/acsomega.3c00754
ACS Omega 2023, 8, 22536−22544

In this work, the characteristic length and diffusion velocity were calculated by MD simulation. From the perspective of the probability distribution, the probability densities of characteristic length and diffusion velocity were statistically calculated. It is found that the probability distributions of characteristic length and diffusion velocity show a trend of increasing and then decreasing, similar to normal distribution. On this basis, the probability density functions of the characteristic length, as shown in eq 8, and the probability density functions of the diffusion velocity, as shown in eq 9, were proposed.

$$F(L) = a\mathrm{e}^{(-b(L-c)^2)} \tag{8}$$

where L is the characteristic length and a, b, and c are the parameters. a and b are related to the standard deviation of the distribution, which indicates the degree of deviation of the data from the mean, and it determines the magnitude of the distribution, and c is the value that occurs most frequently and is the average of the characteristic lengths, which determines the location of the distribution.

$$F(V) = A\mathrm{e}^{(-B(V-C)^2)} \tag{9}$$

where V is the diffusion velocity; A, B, and C are the parameters. A and B are related to the standard deviation of the distribution, which indicates the degree of deviation of the data from the mean, and it determines the magnitude of the distribution, and c is the value that occurs most frequently and is the average of the diffusion velocity, which determines the location of the distribution.

The results of the D_{LV} model and the D_{MSD} model were compared and calculated in the paper. The calculation of relative deviation (R.D.) is based on eq 10.

$$\text{R. D.} = \frac{|D_{LV} - D_{MSD}|}{D_{MSD}} \times 100\% \tag{10}$$

where R.D. is the relative deviation and D_{LV} and D_{MSD} are the diffusion coefficients of the two models.

2.2. Simulation Method. In this study, all simulations were modeled using the COMPASS force field and Amorphous Cell module in Materials Studio software.[37−39] The total potential energy in the COMPASS force field includes the sum of the valence action term, the cross-energy term, and the nonbonded interaction term. The nonbonded interactions in the interaction potential include the Coulomb term describing the electrostatic interactions and the Lennard-Jones potential describing the van der Waals interactions. The liquid system is an infinitely dilute aqueous solution with water molecules modeled by SPC and uses the SHAKE algorithm to constrain the hydrogen bonds. We calculate the diffusion coefficients for SPC water using D_{LV} and D_{MSD}, respectively. The diffusion coefficients of water calculated from the SPC water model used in this paper are in good agreement with the reference values and are calculated to be large compared to SPC/E. This is reflected in many references, as shown in the Table 1 below.

The total number of molecules in the solution system is 561, the number of water molecules is 556, and the number of solute molecules is 5. The gas system is 1000 gas molecules. Taking the alanine and CO_2 system as an example, the simulation box with 556 H_2O and 5 alanine molecules is shown in Figure 1a, and the simulation box with 1000 CO_2 molecules is shown in Figure 1b. The starting configuration of the simulation is a face-centered cubic lattice, and the starting orientation of the molecules is randomly oriented. A simulation box with periodic boundary conditions was used, and the simulation box was replicated infinitely throughout the space to eliminate the boundary effects caused by small samples.[44] The system density was set to match the actual solution density, and the starting velocity of each molecule was sampled according to the Maxwell distribution, and the velocity was subsequently recalibrated to ensure that the total system momentum was zero. For each system, geometric optimization is performed to bring the system to a stable configuration.

Table 1. Diffusion Coefficient of Pure Liquid Water (N: the Number of Particles; T: Temperature)

		D_{MSD} (10^{-9} m^2 s^{-1})		refs
N	T (K)	SPC	SPC/E	
216	298.2	4.02	2.41	40
1000	300.7	4.2	2.4	41
820	301	4.5	2.8	42
2201	298.15	4.29	2.7	43
278	298.15	4.11		this work
		D_{LV} (10^{-9} m^2 s^{-1})		
278	298.15	4.27		this work

For the constructed system, the structure was first geometrically optimized and then run under NPT (1 ns), NVT (1 ns), and NVE (1 ns) conditions, with each simulation starting from the final coordinates and velocities of the previous simulation, and the final diffusion data coming from the results of the NVE ensemble simulation. The integration step in the calculation was chosen to be 1 fs. A Nosé thermostat with a coupling constant of 0.1 and a Berendsen barometer with a coupling constant of 0.5 were used to control the system temperature and pressure, respectively.[45−47] In this study, the van der Waals interaction forces were calculated using the group-based method, and the electrostatic interaction forces were simulated using the Ewald method. The spherical cutoff method was used in the simulations, and the cutoff radius was chosen to be half of the simulation box for the liquid system and 15.5 Å for the gas system calculations.[48,49] After each calculation, a script was used to output the coordinates. To avoid individual simulations without sufficient sampling space, i.e., molecules trapped in local minima or slow dynamics, increasing the number of iterations can help reduce this uncertainty.[50,51] In this paper, 10 iterations of the computational system were performed to obtain better statistics.

The results of molecular dynamics simulations can provide microscopic details of molecular motion, obtaining continuous trajectories over time. The diffusion velocity is the average velocity of the molecular motion, a statistical average velocity derived from the available statistical samples. After a complete kinetic simulation, the instantaneous velocity of each molecule at each step can be obtained directly from the trajectory file by the script. The V of the molecular motion is obtained from the available statistical samples. The characteristic length represents the statistical average of the diffusion distance traveled by the moving molecule without changing its direction. After a complete kinetic simulation, the position coordinates of each molecule at each step can be obtained from the trajectory file. Then, the calculation method proposed by Chen was used to obtain the L of the calculated system molecules.[16]

3. RESULTS AND DISCUSSION

3.1. Characteristic Length and Diffusion Velocity Distribution. After the kinetic simulation, the diffusion velocity

https://doi.org/10.1021/acsomega.3c00754
ACS Omega 2023, 8, 22536−22544

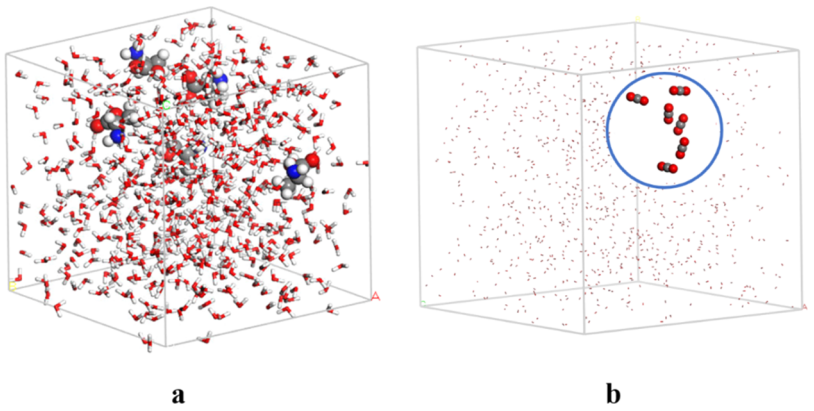

Figure 1. (a) Simulation box for alanine solution system. (b) Simulation box for carbon dioxide system.

Table 2. Parameters of the Characteristic Length Distribution Function

gas systems	*a*	*b*	*c*	r^2	liquid systems	*a*	*b*	*c*	r^2
N_2	0.11	0.0040	248.02	0.96	CH_3OH	0.58	0.50	0.022	0.98
O_2	0.13	0.0087	239.18	0.96	HCOOH	1.07	0.32	0.021	0.97
CO	0.12	0.0068	250.37	0.98	urea	2.11	1.22	0.021	0.99
CO_2	0.15	0.0089	172.49	0.99	glycine	1.62	0.82	0.017	0.99
NH_3	0.13	0.0146	300.51	0.96	alanine	0.26	0.05	0.014	1.00
CH_4	0.16	0.0100	316.19	0.99	valine	2.25	0.56	0.013	0.99
C_2H_2	0.11	0.0074	261.81	0.97	threonine	0.22	0.03	0.014	0.99
C_2H_6	0.12	0.0068	242.93	0.99	leucine	2.35	0.87	0.013	0.99
C_4H_{10}	0.10	0.0060	164.63	0.99	glutamic acid	0.98	0.39	0.010	0.98
C_6H_6	0.14	0.0067	98.27	0.99	arginine	0.19	0.04	0.008	0.96

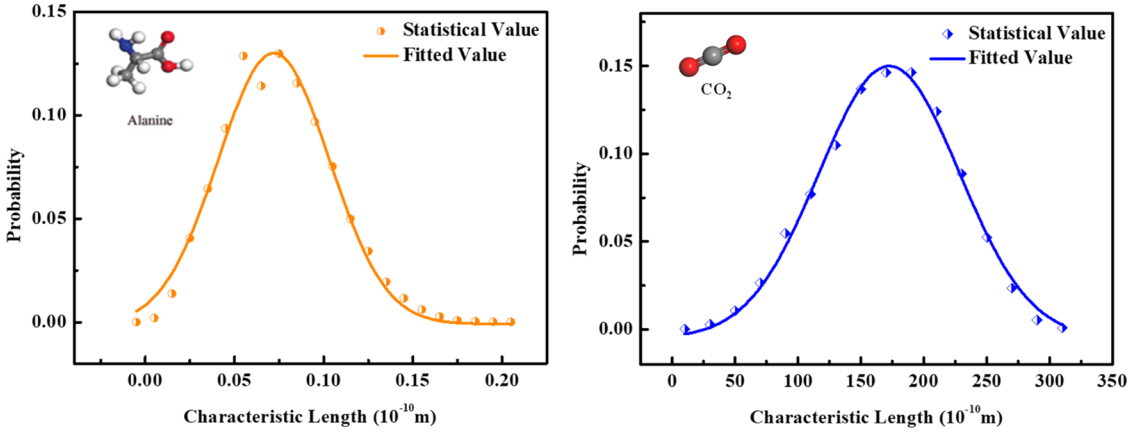

Figure 2. Probability distribution of the characteristic length of alanine and carbon dioxide.

and the complete trajectory of molecular motion can be obtained for each frame by scripting. In this paper, the diffusion process was calculated for 10 gas systems and 10 liquid systems at 1 atm and 298.15 K. The instantaneous velocities of molecular diffusion in all samples were counted, and the characteristic lengths of molecular motion were obtained from the obtained motion trajectories.

In this work, the characteristic length of molecular diffusion is calculated, and the probability density distribution function is obtained by statistical analysis. The model parameters and correlation coefficient values are shown in Table 2. The characteristic length probability distributions of alanine and carbon dioxide were taken as an example, as shown in Figure 2.

As can be seen from Table 2, the minimum value of the model correlation coefficient r^2 is 0.96, and the average value is 0.98, so the distribution function proposed in this paper is accurate for the description of *L*. The distribution function provides a better understanding of the numerical magnitude and probability of occurrence of *L*. Parameters *a* and *b* indicate the degree of deviation of *L* from the average value and determine the width of the distribution function. Parameter *c* is the location of the maximum probability density of *L*, which is the average of the characteristic lengths and is used to calculate the diffusion coefficient in the D_{LV} model. As shown in Figure 2, the probability density points of the molecular characteristic length obey the new distribution function very well. Meanwhile, the characteristic length of the liquid system is much smaller than that of the gas system. This law reflects the difference in the way molecules move in liquid and gas systems. Molecular motion is a random event, and its modes of motion mainly include

https://doi.org/10.1021/acsomega.3c00754
ACS Omega 2023, 8, 22536−22544

Table 3. Parameters of the Distribution Function of Diffusion Velocity

gas systems	A	B	C	R^2	liquid systems	A	B	C	R^2
N_2	0.18	0.13	8.01	0.99	CH_3OH	0.13	0.05	6.93	0.97
O_2	0.16	0.13	7.33	0.99	HCOOH	0.12	0.07	7.24	0.99
CO	0.10	0.12	7.13	1.00	urea	0.14	0.06	6.50	0.96
CO_2	0.16	0.17	7.33	0.98	glycine	0.11	0.07	6.28	0.99
NH_3	0.11	0.15	7.75	0.99	alanine	0.13	0.05	7.38	0.99
CH_4	0.06	0.05	8.21	0.99	valine	0.11	0.09	7.35	0.99
C_2H_2	0.09	0.10	7.58	0.99	threonine	0.12	0.05	7.61	0.99
C_2H_6	0.11	0.15	7.21	0.97	leucine	0.15	0.07	7.49	0.98
C_4H_{10}	0.13	0.12	7.26	0.99	glutamic acid	0.13	0.05	7.56	0.99
C_6H_6	0.12	0.17	7.09	0.99	arginine	0.09	0.05	7.40	0.99

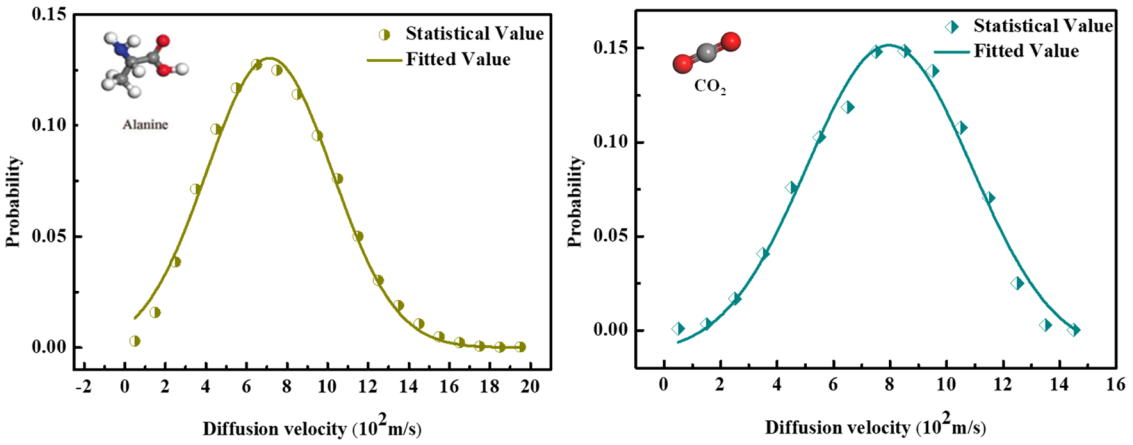

Figure 3. Probability distribution of the diffusion velocity of alanine and carbon dioxide.

Table 4. Calculated Results for Gas Systems

groups	molar mass (g·mol^{-1})	L (10^{-9} m)	V (10^2 m·s^{-1})	D_{LV} (10^{-5} m^2 s^{-1})	D_{MSD} (10^{-5} m^2 s^{-1})	R.D.$_1$ (%)	D_{exp} (10^{-5} m^2 s^{-1})	R.D.$_2$ (%)
CH_4	16	31.62	8.21	2.60 ± 0.03	3.12 ± 0.08	16.79	2.40[53]	8.33
NH_3	17	30.05	7.75	2.33 ± 0.05	2.4 ± 0.04	2.96		
C_2H_2	26	26.18	7.58	1.98 ± 0.05	1.9 ± 0.04	4.44		
CO	28	25.04	7.13	1.79 ± 0.06	2.21 ± 0.05	19.21		
N_2	28	24.80	8.01	1.99 ± 0.05	2.32 ± 0.05	14.38	2.12[53]	6.13
C_2H_6	30	24.29	7.21	1.75 ± 0.09	1.74 ± 0.03	0.65		
O_2	32	23.92	7.33	1.75 ± 0.09	1.97 ± 0.07	11.00	2.32[53]	24.57
CO_2	44	17.25	7.33	1.26 ± 0.03	1.36 ± 0.03	7.03	1.13[53]	11.50
C_4H_{10}	58	16.46	7.26	1.19 ± 0.04	0.98 ± 0.10	21.94		
C_6H_6	78	9.83	7.09	0.70 ± 0.03	0.64 ± 0.08	8.90		
average						10.73		12.63

translation, rotation, and vibration.[52] In gas systems, the molecules are far apart, and the intermolecular space is large, so the intermolecular interaction forces are relatively small. Translational motion contributes significantly to the motion of gas molecules, and gas molecules do not easily change direction, so the characteristic length is large. In contrast, in the liquid system, the molecules are relatively crowded with each other, and the intermolecular forces are large. At this time, the contribution of molecular vibration and rotation to the motion of liquid molecules is larger, and the motion of liquid molecules is more likely to collide with surrounding molecules, leading to a change in the direction of molecular motion, and the characteristic length is smaller. However, the molecular characteristic lengths of both gas and liquid molecules are consistent with our proposed normal-like distribution, indicating that the one-step distance of molecular motion is concentrated in a certain length range.

In this paper, the molecular motion velocity data of various systems were statistically analyzed to obtain the new distribution functions. The parameters of the fitted distribution functions for the diffusion velocities of gas and liquid systems are shown in Table 3. The molecular diffusion velocity distribution of the aqueous alanine solution and carbon dioxide system was taken as an example, as shown in Figure 3.

From Table 3, the minimum value of the model correlation coefficient R^2 is 0.96, and the average value is 0.99, indicating that the new distribution function applies to the distribution of V. As shown in Figure 3, taking alanine and carbon dioxide as examples, it can be found that the probability density points of the molecular motion velocity obey our proposed new distribution function. The parameters A and B indicate the degree of deviation of V from the average value. From the values of A and B in the table, it can be seen that the height and width of the distribution of V are similar for both gas and liquid systems.

https://doi.org/10.1021/acsomega.3c00754
ACS Omega 2023, 8, 22536−22544

Parameter C is the location of the maximum probability density of V, which is the average value of V. It is used to calculate the diffusion coefficient in the D_{LV} model. The high probability event of the average velocity of molecular motion occurs around 7.0×10^2 m^2/s. This indicates that the diffusion velocity of gas and liquid molecules is most likely to be around 7.0×10^2 m^2/s.

3.2. Effect of Molar Mass on Diffusion Velocity and Characteristic Length. The diffusion process is affected by various factors, and the diffusion characteristics are different for substances of different molecular masses. In this paper, 10 gas molecules and 10 liquid molecules were calculated at 298.15 K, 1 atm. The characteristic lengths, diffusion velocities, and diffusion coefficients of the different systems were statistically calculated. The D_{MSD} was obtained from the mean square displacement versus time curves, as shown in Figures S1 and S2. We selected the slope of the well-linearized part of the mean square displacement time plot to calculate the molecular diffusion coefficients and obtained the average value for multiple simulations. The results of the calculations for the different diffusion systems are shown in Tables 4 and 5 (R.D.$_1$ is the relative error of D_{LV} and D_{MSD}, and R.D.$_2$ is the relative error of D_{LV} and experimental data). The molecular molar mass and characteristic length relationships are shown in Figure 4.

It can be seen from Figure 4 that as the molar mass of gas molecules increases, the corresponding characteristic length tends to become smaller. This is because the larger the molecular mass of a gas, the easier it is to change the direction of motion and the smaller the characteristic length. This is also the case for liquid systems. When the molecular molar mass becomes larger, the molecules are more likely to collide with the surrounding molecules during diffusion and change their trajectory. As a result, the molecular one-step displacement distance becomes shorter, and the diffusion coefficient becomes smaller. As can be seen from Tables 4 and 5, there is no obvious pattern in the variation of diffusion rate with molar mass in diffusion systems with different molar masses. Comparing the two sets of diffusion coefficient data for the D_{LV} and D_{MSD} models for the gas system, the minimum relative deviation was 2.96%, and the average relative deviation was 10.73%. The D_{LV} and D_{MSD} corrections were performed for the liquid system by using the Yeh–Hummer correction, the minimum relative deviation after the correction was 0.97%, and the average relative deviation was 12.93%. Since the structure and conditions of the simulations are, strictly speaking, ideal conditions, the actual conditions are perhaps more complex, and therefore the calculated results show errors with the experimental results. The results show that the new model can predict the diffusion coefficient of the molecule. The differences between the D_{LV} and D_{MSD} calculations are mainly due to the different data analysis methods of the two models. D_{LV} obtains the diffusion velocity and characteristic length directly and then obtains the diffusion coefficient. In contrast, the process of calculating the diffusion coefficient by D_{MSD} uses the slope of the MSD to the time curve to calculate, and the calculation of the slope may also have some errors. The results of diffusion coefficients both in the D_{LV} model and the D_{MSD} model tend to decrease with the increase of molecular molar mass. From the definition of the D_{LV} model, it can be further clarified that the effect of different molecular molar masses on diffusion mainly affects its characteristic length of diffusion.

3.3. Effect of Temperature on Diffusion Velocity and Characteristic Length. For the same system, the effect of temperature on the diffusion coefficient is that the higher the

Table 5. Calculated Results for Liquid Systems

groups	molar mass (g·mol^{-1})	cell size (Å)	D_{YH} (10^{-11} m^2 s^{-1})	L (10^{-12} m)	V (10^2 m s^{-1})	D_{LV} (10^{-10} m^2 s^{-1})	D_{MSD} (10^{-10} m^2 s^{-1})	$D_{LV\text{-cd}}$ (10^{-10} m^2 s^{-1})	$D_{MSD\text{-cd}}$ (10^{-10} m^2 s^{-1})	R.D.$_1$ (%)	D_{exp} (10^{-10} m^2 s^{-1})	R.D.$_2$ (%)
CH_3OH	32	23.58	2.92	2.19	6.93	15.18 ± 0.10	19.32 ± 0.09	15.47	19.61	21.13	15.4[54]	0.45
HCOOH	46	23.64	2.86	2.10	7.24	15.20 ± 0.08	18.04 ± 0.13	15.49	18.33	15.48		
urea	60	23.64	2.97	2.10	6.50	13.65 ± 0.07	13.87 ± 11	13.95	14.17	1.55	13.7[55]	1.82
glycine	75	23.76	5.88	1.71	6.28	10.74 ± 0.04	10.63 ± 0.09	11.33	11.22	0.97	10.6[56]	6.89
alanine	89	23.81	2.92	1.43	7.38	10.55 ± 0.11	9.21 ± 0.14	10.85	9.50	14.14	9.3[56]	16.67
valine	117	23.87	7.93	1.31	7.35	9.63 ± 0.12	7.54 ± 0.11	10.42	8.33	25.06	7.8[56]	33.59
threonine	119	23.98	21.34	1.30	7.23	9.40 ± 0.09	7.23 ± 0.08	11.53	9.36	23.16	7.86[55]	45.95
leucine	131	23.99	5.29	1.29	7.49	9.66 ± 0.08	8.44 ± 0.06	10.19	8.97	13.63	7.4[56]	37.70
glutamic acid	147	24.09	8.32	1.00	7.56	7.56 ± 0.04	7.02 ± 0.12	8.39	7.85	6.88	7.4[57]	13.38
arginine	174	24.02	2.28	0.79	7.40	5.85 ± 0.04	5.43 ± 0.07	6.07	5.66	7.35	7.0[55]	13.29
average										12.93		18.86

https://doi.org/10.1021/acsomega.3c00754
ACS Omega 2023, 8, 22536−22544

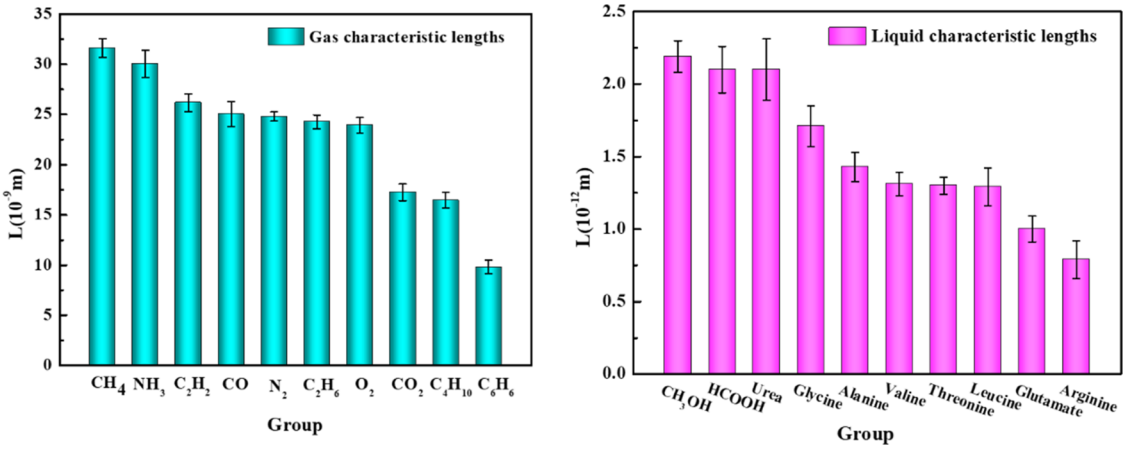

Figure 4. Relationship between molecular molar mass and characteristic length.

Table 6. Calculation Results of CO_2 at Different Temperatures

systems	T (K)	L (10^{-9} m)	V (10^2 m·s^{-1})	D_{LV} (10^{-5} m^2 s^{-1})	D_{MSD} (10^{-5} m^2 s^{-1})	R.D. (%)
CO_2	278.15	17.52	6.92	1.21	1.27	4.72
	298.15	17.25	7.33	1.26	1.36	7.35
	318.15	17.01	7.97	1.36	1.42	4.23
	338.15	18.72	8.08	1.51	1.55	2.58
	358.15	18.23	8.30	1.51	1.61	6.21
average						5.02

Table 7. Calculation Results of Alanine at Different Temperatures

systems	T (K)	L (10^{-12} m)	V (10^2 m·s^{-1})	$D_{LV\text{-}cd}$ (10^{-10} m^2 s^{-1})	$D_{MSD\text{-}cd}$ (10^{-10} m^2 s^{-1})	R.D. (%)
alanine	278.15	1.24	6.98	8.41	8.71	3.72
	298.15	1.43	7.38	10.31	9.24	12.30
	318.15	1.33	7.60	9.93	10.63	6.79
	338.15	1.40	7.84	11.01	11.04	0.22
	358.15	1.41	8.01	11.24	11.50	2.49
average						4.83

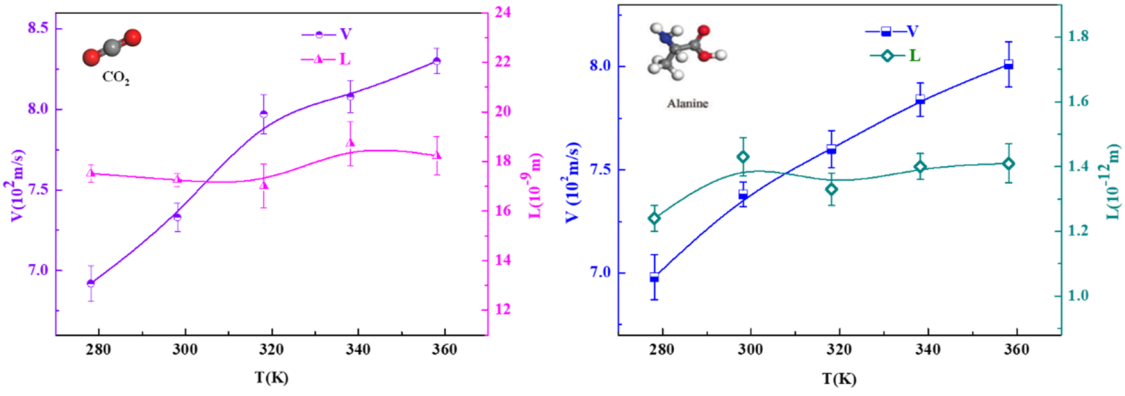

Figure 5. Relationship between different temperatures and diffusion velocity.

temperature, the greater the diffusion coefficient.[58] In this paper, we further investigated the effect of temperature on diffusion from the perspective of the D_{LV} model. The characteristic lengths and diffusion velocities of alanine and carbon dioxide were calculated for five temperatures (278.15, 298.15, 318.15, 338.15, and 358.15 K). The D_{LV} model was also compared with the D_{MSD} calculation results. The calculated results are shown in Tables 6 and 7 and Figure 5.

As shown in Tables 6 and 7 and Figure 5, the average velocity of molecules increases with increasing the temperature of the system, while the temperature does not affect the diffusion distance of molecules. Molecular potential energy is an important driving force of the diffusion process, and increasing the temperature of the system increases the molecular potential energy and accelerates the movement. From the calculated data of D_{LV} and D_{MSD} models, it is known that the diffusion coefficient becomes larger with increasing temperature. According to the D_{LV} model, it is further known that the temperature of the system mainly affects the average speed of molecular diffusion. Meanwhile, the average relative deviation of

https://doi.org/10.1021/acsomega.3c00754
ACS Omega 2023, 8, 22536−22544

the calculated CO_2 D_{LV} and D_{MSD} diffusion coefficients is 5.02%, and that of the calculated alanine $D_{LV\text{-}cd}$ and $D_{MSD\text{-}cd}$ diffusion coefficients is 4.83%, which indicates that the new diffusion coefficient model is accurate.

4. CONCLUSIONS

In this work, 20 diffusion systems were calculated to study the distribution of the parameters L and V of the D_{LV} model. The probability density distribution functions of L and V were obtained by statistical calculations of the data of L and V (the average of the correlation coefficients was 0.98 and 0.99). The distribution range of L and V can be determined by analyzing the parameters of the distribution function, and the expected values of L and V were obtained. The diffusion coefficient data of the D_{LV} and D_{MSD} models for the gas system showed a minimum relative deviation of 2.96% and an average relative deviation of 10.73%, and the average relative deviation of the D_{LV} from the experimental value was 12.63%. The Yeh−Hummer correction method was used to correct the D_{LV} and D_{MSD} for the liquid system, the minimum relative deviation after the correction was 0.97%, the average relative deviation was 12.93%, and the average relative deviation of the D_{LV} from the experimental value was 18.86%. The results indicate that the new model calculations are accurate and reliable. The mechanism of the influence of molecular molar mass and system temperature on the diffusion coefficient was revealed by the D_{LV} model. The results show that the variation of the diffusion coefficient is due to the decrease of the characteristic length with the increase of the molar mass and the increase of the diffusion velocity with the increase of the temperature. This paper provides a new idea to study the nature of diffusion processes and provides a basis for the further understanding of molecular motion.

■ ASSOCIATED CONTENT

Supporting Information

The Supporting Information is available free of charge at https://pubs.acs.org/doi/10.1021/acsomega.3c00754.

Mean square displacement time curve for the gas system and mean square displacement time curve for the solution system (PDF)

■ AUTHOR INFORMATION

Corresponding Author

Lianying Wu − *College of Chemistry and Chemical Engineering, Ocean University of China, Qingdao 266100, China*; Email: wulianying@ouc.edu.cn

Authors

Wenting Sun − *College of Chemistry and Chemical Engineering, Ocean University of China, Qingdao 266100, China*; orcid.org/0009-0007-9817-8542

Xia Chen − *Institute of Chemical Engineering Guangdong Academy of Science, Guangzhou 510665, China*

Yangdong Hu − *College of Chemistry and Chemical Engineering, Ocean University of China, Qingdao 266100, China*; orcid.org/0000-0001-5159-4978

Weitao Zhang − *College of Chemistry and Chemical Engineering, Ocean University of China, Qingdao 266100, China*; orcid.org/0000-0002-0680-9391

Complete contact information is available at: https://pubs.acs.org/10.1021/acsomega.3c00754

Notes

The authors declare no competing financial interest.

■ ACKNOWLEDGMENTS

This work was supported by the National Natural Science Fund Program of China (21776264). The authors' sincere appreciation goes to Prof. Hu and Prof. Wu, for their scientific guidance.

■ REFERENCES

(1) Kerkhof, P. J. A. M.; Geboers, M. A. M. Analysis and extension of the theory of multicomponent fluid diffusion. *Chem. Eng. Sci.* **2005**, *60*, 3129−3167.

(2) Zhao, X.; Luo, T.; Jin, H. A predictive model for self-, Maxwell-Stefan, and Fick diffusion coefficients of binary supercritical water mixtures. *J. Mol. Liq.* **2021**, *324*, 114735−114747.

(3) Meininghaus, R.; Kirchner, S.; Maupetit, F.; Sallee, H.; Quenard, D. Gravimetric studies on VOC adsorption by indoor materials under near-ambient conditions. *Indoor Built Environ.* **2000**, *9*, 277−283.

(4) Bodalal, A.; Zhang, J.; Plett, E. A method for measuring internal diffusion and equilibrium partition coefficients of volatile organic compounds for building materials. *Build. Environ.* **2000**, *35*, 101−110.

(5) Meininghaus, R.; Uhde, E. Diffusion studies of VOC mixtures in a building material. *Indoor Air* **2002**, *12*, 215−222.

(6) Rodrigo, M. M.; Valente, A. J. M.; Barros, M. C. F.; Verissimo, L. M. P.; Ramos, M. L.; Justino, L. L. G.; Burrows, H. D.; Ribeiro, A. C. F.; Esteso, M. A. Binary diffusion coefficients of l-histidine methyl ester dihydrochloride in aqueous solutions. *J. Chem. Thermodyn.* **2015**, *89*, 240−244.

(7) Miller, D. G. The History of Interferometry for Measuring Diffusion Coefficients. *J. Solution Chem.* **2014**, *43*, 6−25.

(8) An, Y.; Althaus, S. M.; Liu, H.-H.; Chen, J.-H. Nuclear magnetic resonance measurement of methane diffusion in organic-rich shales. *Fuel* **2019**, *247*, 160−163.

(9) Artola, P. A.; Rousseau, B. Thermal diffusion in simple liquid mixtures: what have we learnt from molecular dynamics simulations? *Mol. Phys.* **2013**, *111*, 3394−3403.

(10) Kamgar, A.; Hamedi, N.; Mohsenpour, S.; Rahimpour, M. R. Investigation of using different thermodynamic models on prediction ability of mutual diffusion coefficient model. *J. Mol. Liq.* **2017**, *243*, 781−789.

(11) Calderon, C. P. Estimation and Inference of Diffusion Coefficients in Complex Biomolecular Environments. *J. Chem. Theory Comput.* **2011**, *7*, 280−290.

(12) Moggridge, G. D. Prediction of the mutual diffusivity in binary non-ideal liquid mixtures from the tracer diffusion coefficients. *Chem. Eng. Sci.* **2012**, *71*, 226−238.

(13) Kamgar, A.; Bakhtyari, A.; Mohsenpour, S.; D'Agostino, C.; Moggridge, G. D.; Rahimpour, M. R. Mutual diffusion in concentrated liquid solutions: a new model based on cluster theory. *J. Mol. Liq.* **2017**, *232*, 516−521.

(14) Oelkers, E. H. Calculation of diffusion coefficients for aqueous organic species at temperatures from 0 to 350 °C. *Geochim. Cosmochim. Acta* **1991**, *55*, 3515−3529.

(15) Chen, X.; Wang, Y.; Wu, L. Y.; Zhang, W. T.; Hu, Y. D. A new model in correlating and calculating the diffusion-coefficient of electrolyte aqueous solutions. *Fluid Phase Equilib.* **2019**, *485*, 120−125.

(16) Chen, X.; Wang, Y.; Wu, L. Y.; Zhang, W. T.; Hu, Y. D. Testing and validation of a self-diffusion coefficient model based on molecular dynamics simulations. *Chin. J. Chem. Eng.* **2021**, *36*, 138−145.

(17) Humbert, M. T.; Zhang, Y.; Maginn, E. J. PyLAT: Python LAMMPS Analysis Tools. *J. Chem Inf. Model.* **2019**, *59*, 1301−1305.

(18) Jamali, S. H.; Wolff, L.; Becker, T. M.; de Groen, M.; Ramdin, M.; Hartkamp, R.; Bardow, A.; Vlugt, T. J. H.; Moultos, O. A. OCTP: A Tool for On-the-Fly Calculation of Transport Properties of Fluids with the Order-n Algorithm in LAMMPS. *J. Chem Inf. Model.* **2019**, *59*, 1290−1294.

(19) Moultos, O. A.; Orozco, G. A.; Tsimpanogiannis, I. N.; Panagiotopoulos, A. Z.; Economou, I. G. Atomistic molecular dynamics

simulations of H_2O diffusivity in liquid and supercritical CO_2. *Mol. Phys.* **2015**, *113*, 2805−2814.
(20) Orozco, G. A.; Moultos, O. A.; Jiang, H.; Economou, I. G.; Panagiotopoulos, A. Z. Molecular simulation of thermodynamic and transport properties for the H_2O+NaCl system. *J. Chem. Phys.* **2014**, *141*, 234507.
(21) Moultos, O. A.; Tsimpanogiannis, I. N.; Panagiotopoulos, A. Z.; Trusler, J. P. M.; Economou, I. G. Atomistic Molecular Dynamics Simulations of Carbon Dioxide Diffusivity in n-Hexane, n-Decane, n-Hexadecane, Cyclohexane, and Squalane. *J. Phys. Chem. B* **2016**, *120*, 12890−12900.
(22) Moultos, O. A.; Tsimpanogiannis, I. N.; Panagiotopoulos, A. Z.; Economou, I. G. Self-diffusion coefficients of the binary (H_2O + CO_2) mixture at high temperatures and pressures. *J. Chem. Thermodyn.* **2016**, *93*, 424−429.
(23) Michalis, V. K.; Moultos, O. A.; Tsimpanogiannis, I. N.; Economou, I. G. Molecular dynamics simulations of the diffusion coefficients of light n-alkanes in water over a wide range of temperature and pressure. *Fluid Phase Equilib.* **2016**, *407*, 236−242.
(24) Zhao, Y. L.; Feng, Y. H.; Zhang, X. X. Molecular simulation of CO_2/CH_4 self- and transport diffusion coefficients in coal. *Fuel* **2016**, *165*, 19−27.
(25) Rezlerova, E.; Jain, S. K.; Lisal, M. Adsorption, Diffusion, and Transport of C_1 to C_3 Alkanes and Carbon Dioxide in Dual-Porosity Kerogens: Insights from Molecular Simulations. *Energy Fuels* *37*, 492 508. DOI: 10.1021/acs.energyfuels.2c03193.
(26) Higgoda, U. A.; Hellmann, R.; Koller, T. M.; Fröba, A. P. Self-diffusion coefficient and viscosity of methane and carbon dioxide via molecular dynamics simulations based on new ab initio-derived force fields. *Fluid Phase Equilib.* **2019**, *481*, 15−27.
(27) Higgoda, U. A.; Hellmann, R.; Koller, T. M.; Fröba, A. P. Enhancement of the predictive power of molecular dynamics simulations for the determination of self-diffusion coefficient and viscosity demonstrated for propane. *Fluid Phase Equilib.* **2019**, *496*, 69−79.
(28) Klinov, A.; Anashkin, I. Diffusion in Binary Aqueous Solutions of Alcohols by Molecular Simulation. *Processes* **2019**, *7*, 947−953.
(29) Zhang, C.; Yang, X. Molecular dynamics simulation of ethanol/water mixtures for structure and diffusion properties. *Fluid Phase Equilib.* **2005**, *231*, 1−10.
(30) Campo, M. G. Molecular dynamics simulation of glycine zwitterion in aqueous solution. *J. Chem. Phys.* **2006**, *125*, No. 114511.
(31) Zeng, J.; Wang, A.; Gong, X.; Chen, J.; Chen, S.; Xue, F. Molecular Dynamics Simulation of Diffusion of Vitamin C in Water Solution. *Chin. J. Chem.* **2012**, *30*, 115−120.
(32) Tan, J.; Chen, C.; Liu, Y.; Wu, J.; Wu, D.; Zhang, X.; He, X.; She, Z.; He, R.; Zhang, H. Molecular simulations of gas transport in hydrogenated nitrile butadiene rubber and ethylene-propylene-diene rubber. *RSC Adv.* **2020**, *10*, 12475−12484.
(33) Santos, J. R. C.; Abreu, P. E.; Marques, J. M. C. Calculation of diffusion coefficients of pesticides by employing molecular dynamics simulations. *J. Mol. Liq.* **2021**, *340*, 117106−117115.
(34) Celebi, A. T.; Jamali, S. H.; Bardow, A.; Vlugt, T. J. H.; Moultos, O. A. Finite-size effects of diffusion coefficients computed from molecular dynamics: a review of what we have learned so far. *Mol. Simul.* **2021**, *47*, 831−845.
(35) Moultos, O. A.; Zhang, Y.; Tsimpanogiannis, I. N.; Economou, I. G.; Maginn, E. J. System-size corrections for self-diffusion coefficients calculated from molecular dynamics simulations: The case of CO_2, n-alkanes, and poly(ethylene glycol) dimethyl ethers. *J. Chem. Phys.* **2016**, *145*, 074109−174115.
(36) Yeh, I. C.; Hummer, G. System-size dependence of diffusion coefficients and viscosities from molecular dynamics simulations with periodic boundary conditions. *J. Phys. Chem. B* **2004**, *108*, 15873−15879.
(37) Sun, H. COMPASS: An ab initio force-field optimized for condensed-phase applications - Overview with details on alkane and benzene compounds. *J. Phys. Chem. B* **1998**, *102*, 7338−7364.
(38) Yang, J.; Ren, Y.; Tian, A.-m.; Sun, H. COMPASS force field for 14 inorganic molecules, He, Ne, Ar, Kr, Xe, H_2, O_2, N_2, NO, CO, CO_2, NO_2, CS_2, and SO_2, in liquid phases. *J. Phys. Chem. B* **2000**, *104*, 4951−4957.
(39) Bunte, S. W.; Sun, H. Molecular Modeling of Energetic Materials: The Parameterization and Validation of Nitrate Esters in the COMPASS Force Field. *J. Phys. Chem. B* **2000**, *104*, 2477−2489.
(40) Wu, Y.; Tepper, H. L.; Voth, G. A. Flexible simple point-charge water model with improved liquid-state properties. *J. Chem. Phys.* **2006**, *124*, No. 024503.
(41) Glättli, A.; Daura, X.; van Gunsteren, W. F. Derivation of an improved simple point charge model for liquid water: SPC/A and SPC/L. *J. Chem. Phys.* **2002**, *116*, 9811−9828.
(42) van der Spoel, D.; van Maaren, P. J.; Berendsen, H. J. C. A systematic study of water models for molecular simulation: Derivation of water models optimized for use with a reaction field. *J. Chem. Phys.* **1998**, *108*, 10220−10230.
(43) van der Spoel, D.; van Maaren, P. J. The origin of layer structure artifacts in simulations of liquid water. *J. Chem. Theory Comput.* **2006**, *2*, 1−11.
(44) Dawass, N.; Kruger, P.; Schnell, S. K.; Bedeaux, D.; Kjelstrup, S.; Simon, J. M.; Vlugt, T. J. H. Finite-size effects of Kirkwood-Buff integrals from molecular simulations. *Mol. Simul.* **2018**, *44*, 599−612.
(45) Nosé, S. A molecular dynamics method for simulations in the canonical ensemble. *Mol. Phys.* **1984**, *52*, 255−268.
(46) Basconi, J. E.; Shirts, M. R. Effects of Temperature Control Algorithms on Transport Properties and Kinetics in Molecular Dynamics Simulations. *J. Chem. Theory. Comput.* **2013**, *9*, 2887−2899.
(47) Berendsen, H. J. C.; Postma, Jv.; Van Gunsteren, W. F.; DiNola, A.; Haak, J. R. Molecular dynamics with coupling to an external bath. *J. Chem. Phys.* **1984**, *81*, 3684−3690.
(48) Gao, D.; Hong, L.; Wang, J.; Zheng, D. Molecular simulation of gas adsorption characteristics and diffusion in micropores of lignite. *Fuel* **2020**, *269*, 117443−117457.
(49) Ewald, P. P. Die Berechnung optischer und elektrostatischer Gitterpotentiale. *Ann. Phys.* **1921**, *369*, 253−287.
(50) Knapp, B.; Ospina, L.; Deane, C. M. Avoiding False Positive Conclusions in Molecular Simulation: The Importance of Replicas. *J. Chem. Theory Comput.* **2018**, *14*, 6127−6138.
(51) Maginn, E. J.; Messerly, R. A.; Carlson, D. J.; Roe, D. R.; Elliot, J. R. Best practices for computing transport properties 1. Self-diffusivity and viscosity from equilibrium molecular dynamics [article v1. 0]. *Living J. Comp. Mol. Sci.* **2019**, *1*, 6324.
(52) Wang, Z.; Yan, H.; Li, Q. B.; Xu, K. Unified gas-kinetic scheme for diatomic molecular flow with translational, rotational, and vibrational modes. *J. Comput. Phys.* **2017**, *350*, 237−259.
(53) Winn, E. B. The temperature dependence of the self-diffusion coefficients of argon, neon, nitrogen, oxygen, carbon dioxide, and methane. *Phys. Rev.* **1950**, *80*, 1024.
(54) Hao, L.; Leaist, D. G. Binary mutual diffusion coefficients of aqueous alcohols. Methanol to 1-heptanol. *J. Chem. Eng. Data* **1996**, *41*, 210−213.
(55) Ma, Y. G.; Zhu, C. Y.; Ma, P. S.; Yu, K. T. Studies on the diffusion coefficients of amino acids in aqueous solutions. *J. Chem. Eng. Data* **2005**, *50*, 1192−1196.
(56) Umecky, T.; Kuga, T.; Funazukuri, T. Infinite dilution binary diffusion coefficients of several alpha-amino acids in water over a temperature range from (293.2 to 333.2) K with the Taylor dispersion technique. *J. Chem. Eng. Data* **2006**, *51*, 1705−1710.
(57) Ribeiro, A. C. F.; Rodrigo, M. M.; Barros, M. C. F.; Verissimo, L. M. P.; Romero, C.; Valente, A. J. M.; Esteso, M. A. Mutual diffusion coefficients of L-glutamic acid and monosodium L-glutamate in aqueous solutions at T=298.15 K. *J. Chem. Thermodyn.* **2014**, *74*, 133−137.
(58) Zhao, X.; Jin, H. Correlation for self-diffusion coefficients of H_2, CH_4, CO, O_2 and CO_2 in supercritical water from molecular dynamics simulation. *Appl. Therm. Eng.* **2020**, *171*, 114941−114949.

https://doi.org/10.1021/acsomega.3c00754
ACS Omega 2023, 8, 22536−22544